Crystal Structure of an Acylation Transition-State Analog of the TEM-1 β-Lactamase. Mechanistic Implications for Class A β-Lactamases †

ARTICLE *in* BIOCHEMISTRY · MARCH 1998

Impact Factor: 3.02 · DOI: 10.1021/bi972501b · Source: PubMed

3 AUTHORS, INCLUDING:

Laurent Maveyraud
Paul Sabatier University - Toulouse III
38 PUBLICATIONS **1,353** CITATIONS

SEE PROFILE

Crystal Structure of an Acylation Transition-State Analog of the TEM-1 β-Lactamase. Mechanistic Implications for Class A β-Lactamases†

Laurent Maveyraud,‡,§ R. F. Pratt,|| and Jean-Pierre Samama*,§

Groupe de Cristallographie Biologique, Institut de Pharmacologie et de Biologie Structurale, UPR 9062 CNRS, 205 route de Narbonne, 31077 Toulouse, France, and Department of Chemistry, Wesleyan University, Middletown, Connecticut 06459

Received October 9, 1997; Revised Manuscript Received December 11, 1997

ABSTRACT: The crystal structure of a phosphonate complex of the class A TEM-1 β-lactamase has been determined to a resolution of 2.0 Å. The phosphonate appears stoichiometrically at the active site, bound covalently to Ser70Oγ, with one phosphonyl oxygen in the oxyanion hole. Although the overall structure is very similar to that of the native enzyme (rms difference 0.37 Å for all heavy atoms), changes have occurred in the position of active site functional groups. The active site is also not in the conformation observed in the complex of another class A β-lactamase, that of *Staphylococcus aureus* PC1, with the same phosphonate [Chen, C. C. H., *et al*. (1993) *J. Mol. Biol. 234*,165−178]. Both phosphonate structures, however, can be seen to represent models of acylation transition-states since in each the deacylating water molecule appears firmly bound to the Glu166 carboxylate group. The major difference between the structures lies in the positioning of Lys73Nζ and Ser130Oγ. In the *S. aureus* structure, the closest interaction of these functional groups is between Lys73Nζ and Ser70Oγ (2.8 Å), while in the TEM-1 structure it is between Ser130Oγ and the second phosphonyl oxygen of the bound inhibitor (2.8 Å). The former structure therefore may resemble a transition state for formation of the tetrahedral species in acylation by nucleophilic attack on the substrate, where Lys73Nζ presumably catalyzes the reaction as a general base. The TEM-1 structure can then be seen as an analogue of the transition state for breakdown of the tetrahedral species, where Ser130Oγ is acting as a general acid, assisting the departure of the leaving group. The class A β-lactamase crystal structures now available lead to a self-consistent proposal for a mechanism of catalysis by these enzymes.

The class A β-lactamases are an extremely important source of bacterial resistance to β-lactam antibiotics. Among the class A enzymes, that of the TEM plasmid is particularly troublesome in view of its proven ability to readily mutate into forms capable of catalyzing the hydrolysis of late-generation β-lactams and of resisting the currently employed β-lactamase inhibitors (*1*). The catalytic apparatus at the active site of the TEM-1 β-lactamase has been revealed by X-ray crystallography (*2*, *3*) and the perturbations of it produced by natural mutants discussed (*4*).

The mechanism of class A β-lactamase catalysis involves a double displacement mechanism (Scheme 1) with an acyl-enzyme intermediate and where the nucleophile is provided by Ser70 (*5*). This mechanism implies the successive formation and breakdown of two anionic tetrahedral species;

Scheme 1

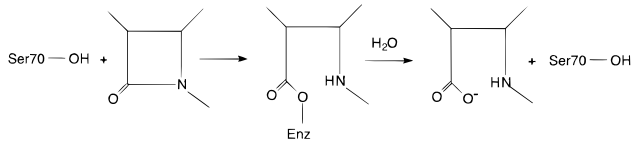

hence, four transition states are passed through during the complete reaction. The current consensus with respect to the active site residues directly contributing to catalysis includes Ser70, Lys73, Ser130, and Glu166; Lys234 and Arg244 are also believed to act as electrostatic catalysts. It is also now generally agreed that the Glu166 carboxylate is the general-base catalyst of the deacylation step where an occluded water molecule, observed directly adjacent to the carboxylate in crystal structures (*3*, *6*), is believed to be the nucleophile. There is much less agreement concerning the mechanism of the acylation step where various general acid/base roles have been attributed to Lys73, Ser130, and Glu166 (*2*, *5*, *7*−*9*). The investigation of a wide range of mutants of these residues (*10*) has not yet led to consensus.

In principle, the crystal structure of a class A β-lactamase with a transition-state analogue bound at the active site would be expected to clarify the roles of these functional groups. One would expect, for a good mimic of the transition state, that the active site functional groups would be disposed around the reaction center in an analogous fashion to that

† This work was supported by the National Institutes of Health (NIH), by the French Ministry of Education (ACC-SV5), and by the Region Midi-Pyrénées.

* To whom correspondence should be addressed at Groupe de Cristallographie Biologique, IPBS-CNRS, 205 route de Narbonne, 31077 Toulouse, France. Tél (switch board): 33 5 61 17 59 00. Tél (direct): 33 5 61 17 54 44. Fax (direct): 33 5 61 17 54 48. E-mail: samama@ipbs.fr.

‡ Present address: Institut für Organische Chemie und Biochemie, Albert-Ludwigs-Universität, Alberstrasse-21, D-79104 Freiburg-im-Breisgau, Germany.

§ Institut de Pharmacologie et de Biologie Structurale.

|| Wesleyan University.

S0006-2960(97)02501-4 CCC: $15.00
Published on Web 02/06/1998

Scheme 2

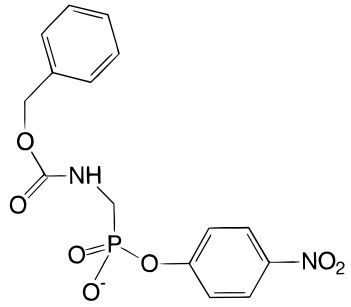

around a transition state of normal catalysis. Indeed, the crystal structure of a boronate complex of the TEM-1 β-lactamase shows the Glu166 carboxyl group directly hydrogen-bonded to one hydroxyl of the boronate as would be expected in a deacylation transition state where Glu166 carboxylate participates as a general-base catalyst of water attack (*11*).

Another crystal structure of a potential transition-state analogue of a class A β-lactamase is also available, that of a phosphonate derivative of the *Staphylococcus aureus* PC1 enzyme (*12*). This structure should also be a good representation of a transition state, as demonstrated by application of the appropriate thermodynamic criterion (*13*). Although the phosphonate moiety in this complex does not contain a leaving group analogue, the hydrolytic water molecule mentioned above does still appear to accompany Glu166, and therefore the structure is probably best interpreted in terms of an acylation transition state (*12, 13*). A detailed analysis of this structure in terms of mechanism has not, however, yet been made. To better understand the relationship between this phosphonate structure and the class A β-lactamase mechanism, a crystal structure of the same phosphonate and the TEM-1 β-lactamase has now been obtained. This structure is significantly different from the *S. aureus* structure with respect to disposition of active site functional groups. We show in this paper how the two structures can be interpreted in terms of a complete and self-consistent acylation mechanism for class A β-lactamases.

MATERIALS AND METHODS

TEM-1 β-lactamase crystals were prepared as previously described (*14*), and stabilized by a stepwise increase of the ammonium sulfate concentration up to 50% saturation. Crystals were mounted in Lindeman glass capillaries with mother liquor, and soaked with a 15 mM solution of *p*-nitrophenyl [N-(benzyloxycarbonyl)aminomethyl]phosphonate (Scheme 2) in 20 mM phosphate buffer, pH 7.8, containing 50% of saturated ammonium sulfate. The final inhibitor concentration was 8 mM, and soaking was pursued for 50 h. Data collection started immediately after the removal of the soaking solution.

Diffraction data were collected at 4 °C on a RaxisII detector, with CuKα X-rays generated from a Rigaku RU300 rotating anode equipped with a Yale double mirror monochromating device. Data were processed with the Rigaku Process software (*15*). Ten percent of the recorded data were randomly selected for R_{free} calculations (*16*). Refinement was performed with X-PLOR 3.1 (*17*). Structures and electron density maps were displayed using the program O (*18*). Rigid-body refinement was first applied, using the 1.8 Å refined native structure as a model (*3*), followed by a refinement cycle using all data between 8.0 and 2.0 Å resolution (simulated annealing from 3000 to 300 K, energy minimization, and individual temperature factor refinement). A phosphonylated serine residue was built and optimized with the program PCMODEL (Serena software, Bloomington, IN), and was used for generating parameters and topology files for X-PLOR. Bond angles and lengths were checked against average values obtained from similar structures in the Cambridge Structural Database (*19*). The phosphonate derivative was introduced in the model at that stage, together with water molecules, when they appeared as positive peaks higher than four standard deviations in difference Fourier electron density maps. Five additional refinement cycles (simulated annealing from 600 to 300 K, followed by positional refinement and individual isotropic *B* factors refinement) using all data between 8.0 and 2.0 Å resolution, intertwined with manual corrections, led to the final structure. The overall occupancy of the bound inhibitor was refined in the last refinement cycle.

Table 1: Data Processing Statistics

	overall resolution range (30.0−2.0 Å)	highest resolution shell (2.25−2.0 Å)
number of observations	38707	5911
number of independent reflections	14698	3909
multiplicity	2.9	2.0
completeness (%)	93.5	86.2
R_{merge} (%)	6.3	14.4
$\langle F/\sigma F \rangle$	20.9	11.9

RESULTS

Structure Refinement. The diffracted intensities to 2.0 Å resolution were measured on a single crystal (Table 1). Rigid-body refinement was performed, using data between 7.0 and 3.0 Å resolution, to take into account the lack of isomorphism between native and enzyme−inhibitor crystals (cell parameters: $a = 42.0$ Å, $b = 63.6$ Å, $c = 89.6$ Å and $a = 42.0$ Å, $b = 60.8$ Å, $c = 88.9$ Å, respectively, in space group $P2_12_12_1$). The $(3F_{obs} - 2F_{calc})$, Φ_{calc} electron density map computed between 8.0 and 2.0 Å resolution, after the first refinement cycle (the R and R_{free} values were 0.235 and 0.284, respectively), showed a continuous density in the active site, extending from Ser70 Oγ (Figure 1a, top). All atoms of the inhibitor, except the *p*-nitrophenyl moiety, which is released during the phosphonylation reaction, were introduced at that stage. The refined structure of the complex includes all protein atoms, the phosphonate ester covalently attached to Ser70Oγ, and 127 water molecules. The final electron density around the inhibitor is shown in Figure 1b (bottom). The final R and R_{free} values for all reflections between 8.0 and 2.0 Å resolution were 0.156 and 0.206, respectively. The overall isotropic temperature factor of all atoms in the structure was 28.9 Å^2, close to the value estimated from Wilson statistics (26.6 Å^2) (*20*). The refined occupancy of the phosphonate inhibitor was 1.0, with an average temperature factor of 29.0 Å^2. The rms coordinate error was estimated from a σ_A plot to be 0.2 Å (*21*).

Structure Description. The overall structure of the protein in the complex is nearly identical with that of the native

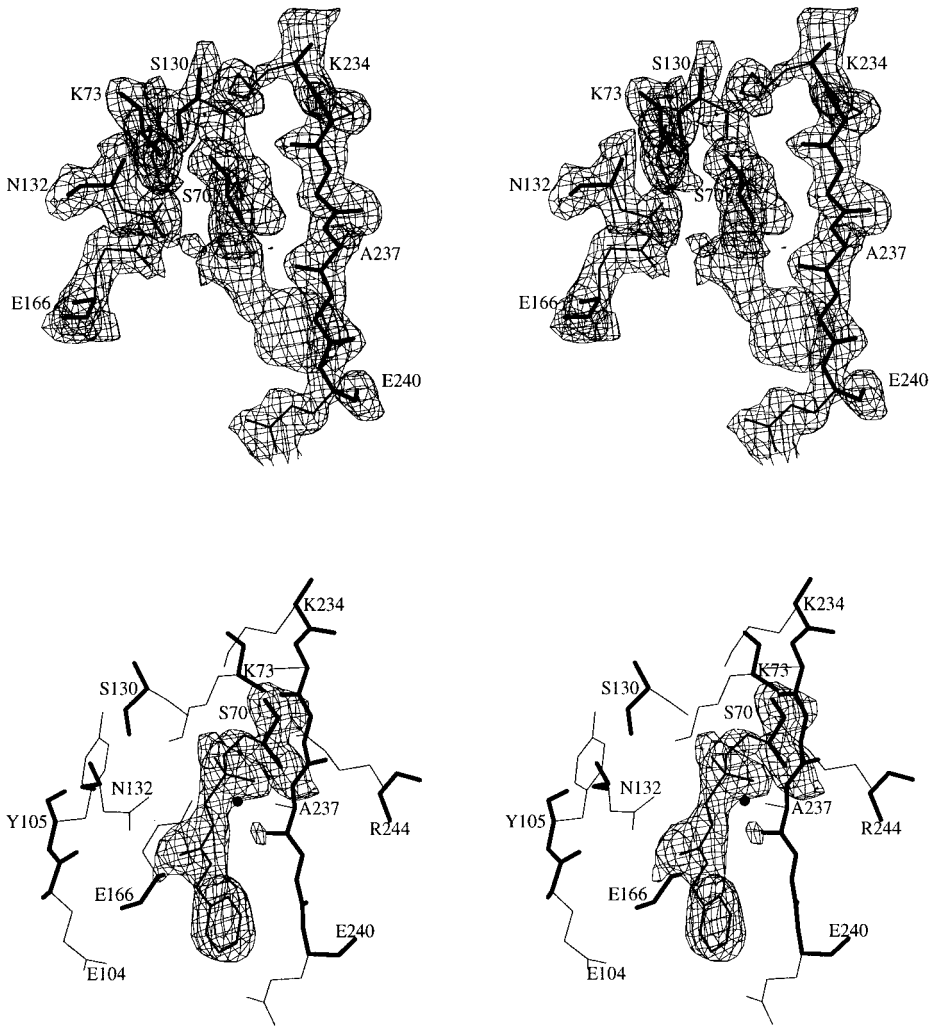

FIGURE 1: (a, top) ($3F_{obs} - 2F_{calc}$) electron density map computed after the first refinement cycle and contoured at 1σ above the mean electron density value. The density extending from Ser70Oγ accounts for all the atoms of the phosphonate moiety. (b, bottom) final ($2F_{obs} - F_{calc}$) electron density map, contoured at 1σ, together with the refined structure. The catalytic water molecule is represented by a filled circle. Thick lines, main-chain atoms; thin lines, side-chain atoms. This figure was generated with Molscript (*33*).

Table 2: Distances Observed in Class A β-Lactamase X-ray Structures (Å)

	apo-enzyme	transition-state analogs of acylation		acyl-enzyme complexes		transition-state analog of deacylation
	TEM−1[a]	TEM-1−phos[b]	PC1−phos[c]	TEM-1−6α[e]	E166N−PenG[f]	TEM-1−bor[d]
S70Oγ−K73Nζ	2.9	3.2	2.8	3.1	3.3	2.8
S70Oγ−H_2O deacyl	2.7	3.1	3.4	2.8	NC[g]	2.4 (OH2)
S70Oγ−Ser130Oγ	3.5	2.9	3.2	3.2	3.3	4.2
E166Oϵ1−H_2O deacyl	2.8	2.7	2.8	2.6	−	2.5 (OH2)
N170Oδ1 −H_2O deacyl	2.8	2.7	3.1	2.7	NC	2.7 (OH2)
E166Oϵ1−K73Nζ	3.4	3.7	2.6	3.8	−	3.2
K73Nζ−S130Oγ	4.2	3.0	4.1	3.0	2.8	4.5
A237N−ligand atom	2.9 (water)	2.9 (O2)	2.9 (O2)	2.8 (O1)	2.7 (O8)	3.0 (OH1)
S70N−ligand atom	3.4 (water)	2.9 (O2)	2.9 (O2)	2.8 (O1)	3.0 (O8)	2.7 (OH1)
S130Oγ−ligand atom		2.8 (O1)	3.3 (O1)	3.1 (N7)	3.1 (N4)	

[a] TEM-1 refined structure (*3*). [b] TEM-1−phosphonate complex (this work). [c] PC1−phosphonate complex (*12*). [d] TEM-1−boronate complex (*11*). [e] TEM-1−6α-(hydroxymethyl)penicillanate complex (*22*). [f] E166N TEM-1−penicillin G complex (*2*). [g] NC, distance not communicated in the original paper.

enzyme. A global superposition of both structures, based on all Cα atoms, led to a rms deviation of 0.37 Å for all protein atoms. The catalytic serine 70 is phosphonylated by the inhibitor (Figures 1b and 2). The phosphonate lies in the substrate binding site and forms a number of hydrogen bonds with the protein which replace those formed by water in the native enzyme (Table 2). The oxygen atom O2 of the inhibitor occupies the oxyanion hole, at 2.9 Å to the main-chain nitrogen atoms of residues 70 and 237. The second oxygen atom bound to phosphorus, O1, is located at 2.8 Å to the hydroxyl group of Ser130 and at 3.4 Å to a water molecule, in a position which is nearly identical with that of the nitrogen atom of the β-lactam ring in acyl-enzyme complexes (*2*, *22*). The nitrogen (N2) and the oxygen (O42)

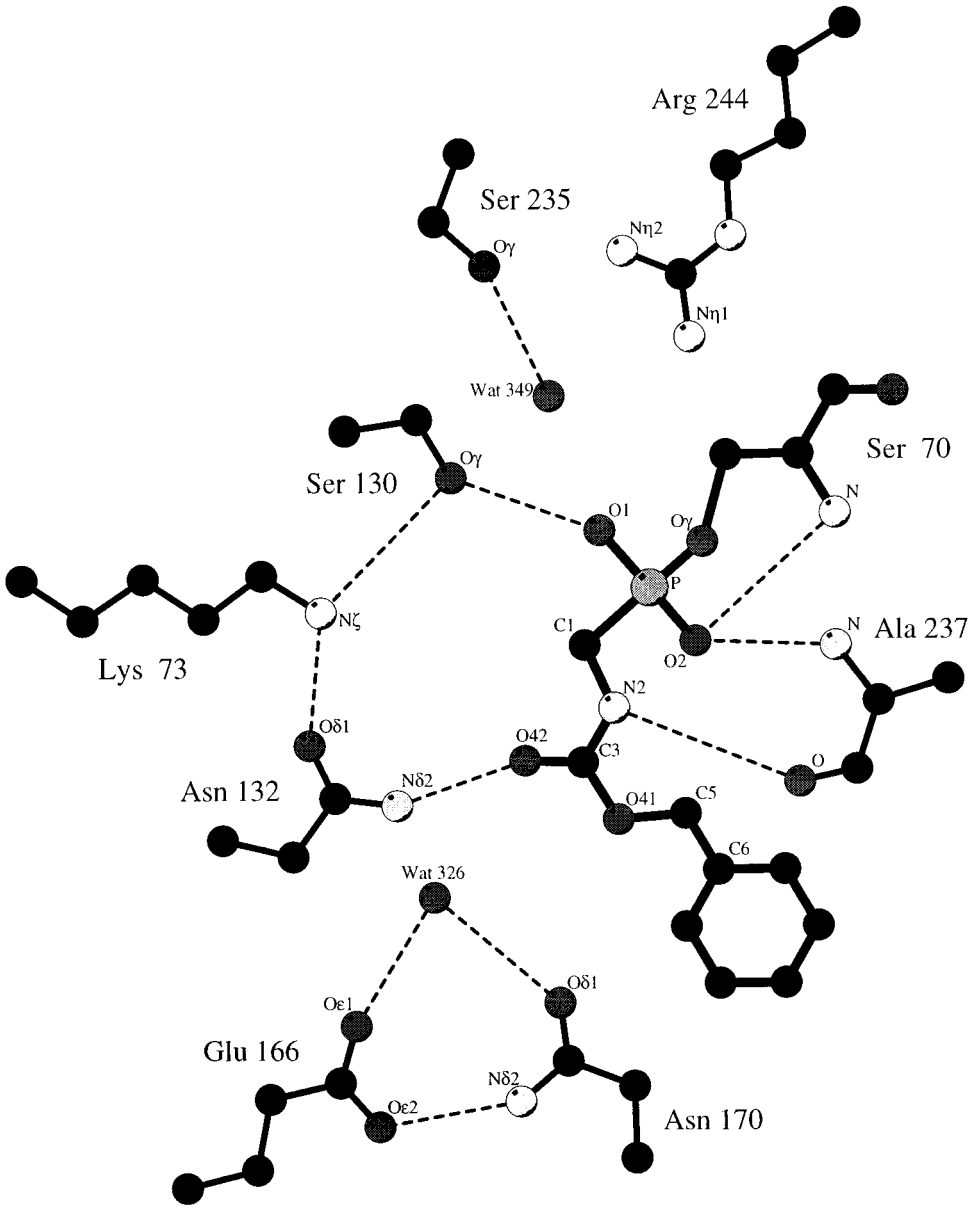

FIGURE 2: Schematic representation of the polar interactions (interatomic distances ≤3.0 Å, dashed lines) observed in the active site of the enzyme. The nomenclature used throughout this article for the phosphonate atoms is given. This figure was generated using Ligplot (*34*).

atoms of the amide group of the inhibitor form hydrogen bonds (3.0 Å) to the main-chain oxygen atom of Ala237 and to the side-chain amide nitrogen atom of Asn132, respectively. Similar interactions were also found between the 6β-acylamido substituent of benzylpenicillin and the E166N mutant of the TEM-1 enzyme in an acyl-enzyme complex (*2*). Finally, the O41 oxygen atom of the phosphonate moiety makes no interaction with protein atoms, and the aromatic ring of the inhibitor is at van der Waals distance to the main-chain atoms of glutamate 240.

Compared to the native structure, some side chains of the active site residues have reoriented upon phosphonate binding (Figure 3) (Table 2). The serine 130 hydroxyl group has moved by 0.6 Å in order to form a hydrogen bond (2.8 Å) with the O1 atom (shown in Figure 2). A similar displacement was also observed in the structure of the TEM-1-6-α-(hydroxymethyl)penicillanic acid complex (*22*) and in the benzylpenicillin−E166N TEM-1 acyl-enzyme complex (*2*) where a hydrogen bond (3.1 Å) was established between Ser130Oγ and the nitrogen atom of the β-lactam ring. The lysine 73 amino group is also displaced by 0.6 Å in the phosphonate complex. The nitrogen atom is at 3.2 Å to Ser70Oγ whereas these groups were at 2.9 Å from each other in the native enzyme. The movements of the serine 130 and lysine 73 side chains bring them to hydrogen bonding distance in the TEM-1−phosphonate complex (3.0 Å). This also occurred upon binding of the 6-α-(hydroxymethyl)-penicillanic acid to the enzyme, and an even tighter hydrogen bond (2.8 Å) was established in the benzylpenicillin−acyl-enzyme complex. This is a significant difference when compared to the native enzyme where the distance between Lys73Nζ and Ser130Oγ is 4.2 Å. The deacylating water molecule, which is considered to be the nucleophilic agent responsible for acyl-enzyme hydrolysis (*2, 5, 7*−*9*), is found at 2.7 Å to the Glu166Oϵ1 and to the Asn170Oδ1 atoms. It is shifted by 0.8 Å compared to its position in the native enzyme, but its interactions with Glu166 and Asn170 are preserved by the 0.5 Å displacement of these side chains.

The structure of the PC1 β-lactamase from *Staphylococcus aureus*, complexed with the same phosphonate derivative,

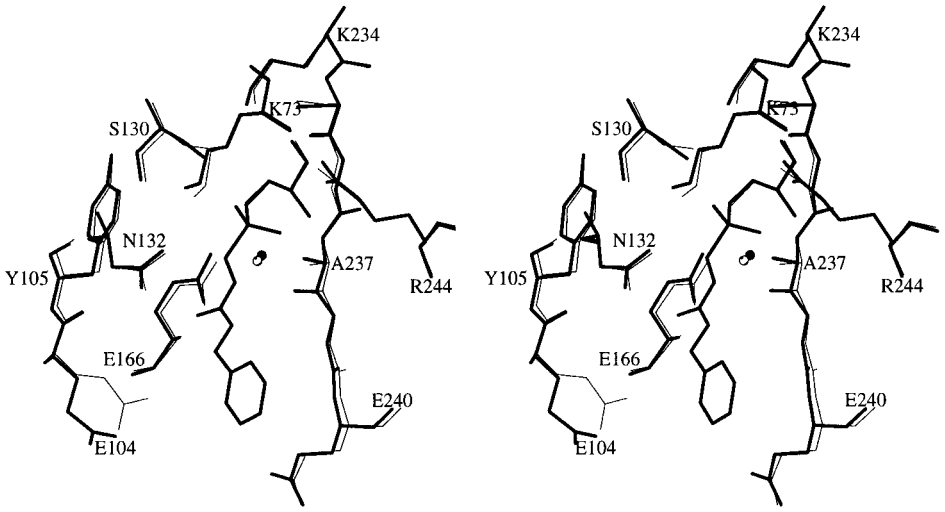

FIGURE 3: Comparison of the active sites in the apo TEM-1 β-lactamase (thin lines) and in the complex with phosphonate (thick lines). The catalytic water molecule is represented by an empty circle for the apo-enzyme, and with a filled circle for the complex. Superposition of both structures is based on all Cα atoms.

was solved at 2.3 Å resolution (*12*). Except for the oxygen atom bound in the oxyanion hole, the set of distances given in Table 2 and illustrated in Figure 4A suggest that the two enzyme−phosphonate complexes are not equivalent species.

DISCUSSION

The networks of hydrogen bonding interactions in the active site, observed in transition-state complexes, should mimic the situation that occurs during catalysis, and may suggest the proton transfer pathways. The crystal structures of the TEM-1 and PC1 enzymes with bound phosphonate appear relevant in that respect. It seems likely that these complexes represent good analogues of a transition state for acyclic depsipeptide hydrolysis (*23*). It has been shown that the β-lactamase-catalyzed hydrolysis of depsipeptides follows a mechanism similar to that of β-lactams (*24*−*26*), and that the thermodynamic properties of the PC1−phosphonate complex were those of a transition-state analogue (*13*).

The phosphonate−enzyme complexes present many of the features that may be expected to occur in the tetrahedral transition states of the catalytic reaction with β-lactam substrates for the following reasons: (1) the position of the O2 oxygen atom in the oxyanion hole is identical with that of the ester carbonyl oxygen in acyl-enzyme complexes; (2) the position of the O1 atom is similar to that of the nitrogen atom of the β-lactam ring; (3) the type of interactions made by the amide group of the phosphonate (N2 and O42) with protein atoms mimics those made by the 6β-acylamido substituents of penicillins. With respect to the catalytic reaction, the phosphonate−enzyme complexes should represent the acylation transition states since the deacylating water molecule is still present in the vicinity of the carboxylate group of Glu166.

The enzymatic hydrolysis of the amide bond proceeds through the sequential formation of the four tetrahedral transition states illustrated in Scheme 3. The first two represent the acylation step. Uptake of the proton from the hydroxyl group of Ser70, assisted by the base B1, is followed by protonation of the nascent amide anion by the proton donor B2 and leads to the acyl-enzyme intermediate. The nature of B1 has been controversial, and three candidates have been proposed: the unprotonated lysine 73 (*2, 9, 27*), the deacylating water molecule activated by Glu166 (*8, 28*), and the Glu166 carboxylate itself (*29*−*31*). In view of the crystal structures now available, the latter possibility, which will not be addressed further in this paper, can only be correct if solution structures differ from the crystal structures by movement of the side chains of the above residues (*32*).

The different sets of interactions observed in the TEM-1− and PC1−phosphonate complexes suggest that each of them represents one of the tetrahedral transition-states species occurring in acylation (Figure 4A,B). In the PC1 enzyme, the distance of Ser130Oγ to both the Lys73Nζ and the O1 atoms is large, 4.1 and 3.3 Å, respectively. The deacylating water molecule is 3.4 Å away from Ser70Oγ, and the only group at hydrogen bonding distance to Ser70Oγ is Lys73Nζ (2.8 Å). These interactions suggest that the PC1−phosphonate complex may correspond to the transition state shown in Figure 4A, where the proton of the serine 70 hydroxyl group is abstracted, and that base B1 is Lys73. The interactions in the TEM-1−phosphonate complex are quite different (Figure 4B) and would agree with the description of the second transition state. Indeed, Ser130Oγ is now at 2.8 Å to the O1 atom and at 3.0 Å to Lys73Nζ, which is at 3.2 Å to Ser70Oγ. Ser130Oγ would thus be well positioned for the concerted delivery of a proton to the leaving nitrogen atom of the β-lactam (located at the O1 position) and for proton uptake from the ammonium group of Lys73. This hydrogen bond pattern suggests Ser130 as the catalytic residue B2, as initially suggested from modeling studies (*8*).

The distance between glutamic acid 166 and lysine 73 varies from 2.6 to 3.7 Å in transition-states A and B, respectively. This variation is significant and may be related to the protonation state of Lys73. The short distance between Lys73 and Glu166 in transition-state A observed in the PC1−phosphonate complex suggests a salt-bridge interaction between the protonated lysine and the carboxylate group. This interaction would strengthen as transition-state A formed, by proton transfer to Lys73Nζ. In transition-state B, where the β-lactam C−N bond is breaking, the basicity of the proton acceptors ranks in the following order: leaving group amide ion ($-NR_1R_2$) > alkoxide (Ser130Oγ) > amine

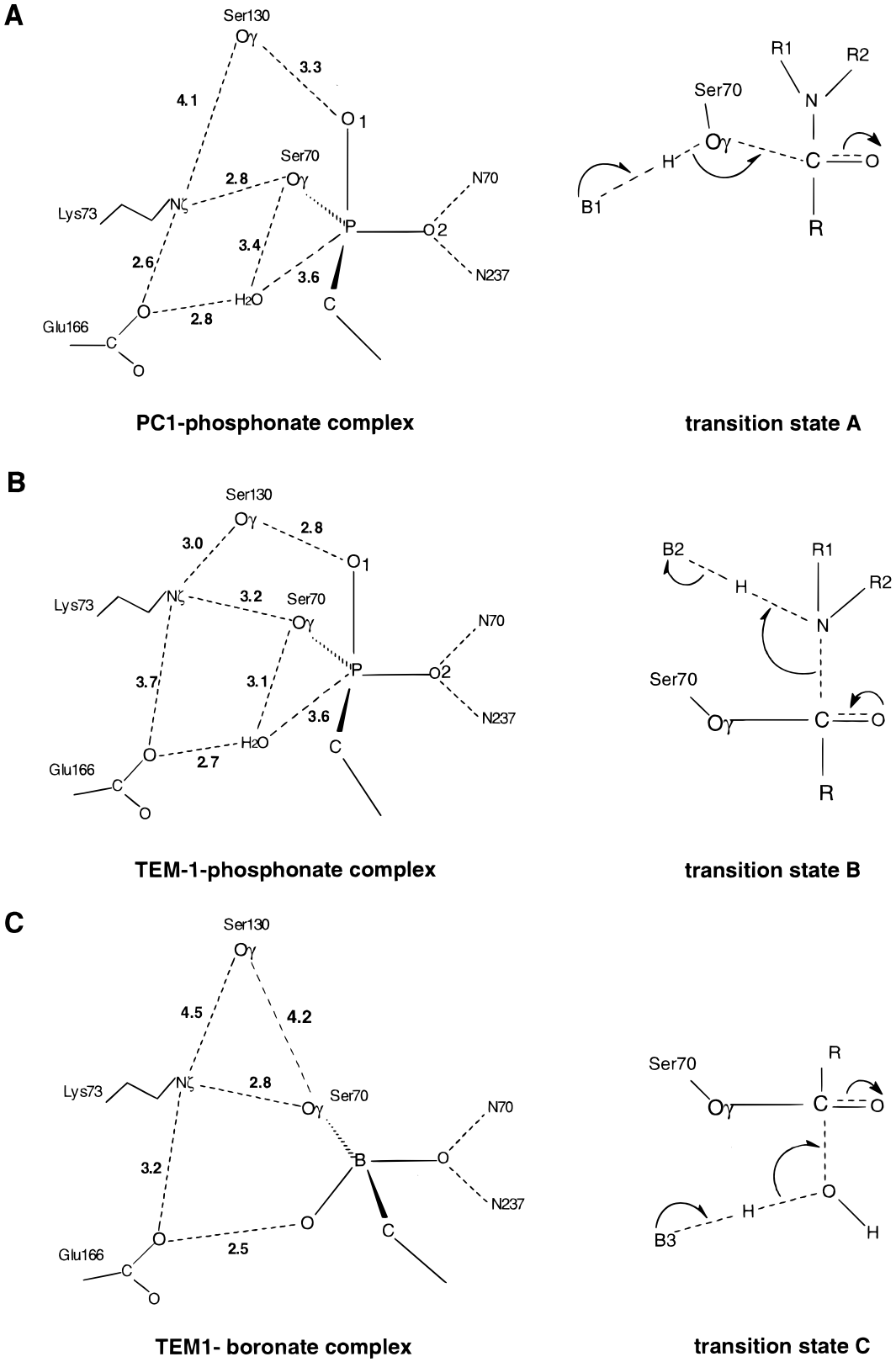

FIGURE 4: Hydrogen bond interactions observed in (A) the PC1−phosphonate complex (*12*), (B) the TEM-1−phosphonate complex (this work), and (C) the TEM-1−boronate complex (*11*).

(Lys73Nζ). Proton transfer in this transition state to the most basic center from the least via Ser130Oγ could explain the close proximity of these groups in the TEM-1−phosphonate complex; the decreasing positive charge on Lys73Nζ in transition-state B would lead to its less favorable interaction with the Glu166 carboxylate, and hence perhaps to the large distance (3.7 Å) between these functional groups in this structure. If the highest energy transition state is the most strongly bound and is thus the most likely represented in the phosphonate structures, one could speculate that the reason for the difference between the PC1− and the TEM-1−phosphonate structures arises from a different rate-

Scheme 3

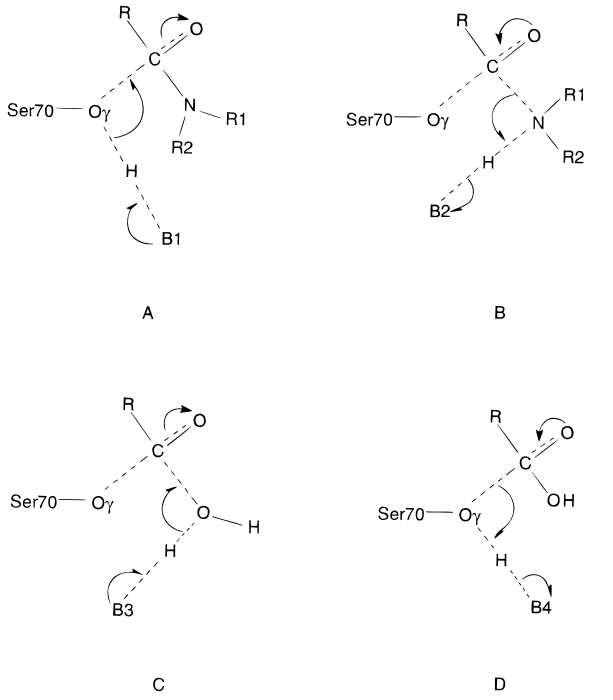

determining step in the respective acylation reactions. Formation of the tetrahedral species would thus be rate-determining in the PC1-catalyzed acylation while breakdown of this species would be rate-determining for acylation of TEM-1.

In the transition states of the deacylation reaction (Scheme 3, C and D), the catalytic water molecule which hydrolyzes the acyl-enzyme intermediate should be replaced by one of the oxygen atoms of the inhibitor. The recently solved crystal structure of the TEM-1−boronate complex (*11*) is a model of such a transition state. According to the 2.5 Å distance between the Glu166Oϵ1 and the oxygen atom on the boron, which displaces the deacylating water molecule, this complex may correspond to the transition state shown in Figure 4C where Glu166 should be the catalytic residue B3.

As demonstrated above, the X-ray structures of class-A β-lactamases with bound phosphonate and boronate transition-state analogues can be interpreted in terms of a complete picture of the catalytic pathway. These complexes, along with those of acyl-enzymes, suggest that central catalytic roles are certainly played by Ser70, Lys73, Ser130, and Glu166. The Lys73 side chain, perhaps depending on its protonation state, moves between Glu166 and Ser130 through side-chain dihedral angle changes. The Lys73Nζ, if neutral, certainly gets close enough to Ser70Oγ for proton abstraction in the first acylation transition state and to regenerate Ser70 for complete deacylation. There remain questions of the state of protonation of the functional groups in the Michaelis ("pre-catalytic") complex and on the degree of mobility of these groups prior to and during catalysis.

ACKNOWLEDGMENT

p-Nitrophenyl [*N*-(benzyloxycarbonyl)aminomethyl]phosphonate was prepared by Dr. Jubrail Rahil at Wesleyan University.

REFERENCES

1. Medeiros, A. A. (1997) *Clin. Infect. Dis. 24 (Suppl. 1)*, S19−S45.
2. Strynadka, N. C. J., Adachi, H., Jensen, S. E., Johns, K., Sielecki, A., Betzel, C., Sutoh, K., and James, M. N. G. (1992) *Nature 359*, 700−705.
3. Jelsch, C., Mourey, L., Masson, J.-M., and Samama, J.-P. (1993) *Proteins: Struct., Funct., Genet. 16*, 364−383.
4. Knox, J. R. (1995) *Antimicrob. Agents Chemother*. *39*, 2593−2601.
5. Waley, S. G. (1992) in *The chemistry of β-lactams* (Page, M. I., Ed.) Chapter 6, Chapman and Hall, London.
6. Herzberg, O., and Moult. J. (1987) *Science 236*, 694−701.
7. Herzberg, O., and Moult. J. (1990) *Curr. Opin. Struct. Biol. 1*, 946−953.
8. Lamotte-Brasseur, J., Dive, G., Dideberg, O., Charlier, P., Frère, J.-M., and Ghuysen, J.-M. (1991) *Biochem. J. 279*, 213−221.
9. Swarén, P., Maveyraud, L., Guillet, V., Masson, J.-M., Mourey, L., and Samama, J.-P. (1995) *Structure 3*, 603−613.
10. Matagne, A., and Frère, J.-M. (1995) *Biochim. Biophys. Acta 1246*, 109−127.
11. Strynadka, N. C. J., Martin, R., Jensen, S. E., Gold, M., and Jones, J. B. (1996*) Nat. Struct. Biol. 3*, 688−695.
12. Chen, C. C. H., Rahil, J., Pratt, R. F., and Herzberg, O. (1993) *J. Mol. Biol. 234*, 165−178.
13. Rahil, J., and Pratt, R. F. (1994) *Biochemistry 33*, 116−125.
14. Jelsch, C., Lenfant, F., Masson, J.-M., and Samama, J.-P. (1992) *J. Mol. Biol. 223*, 377−380.
15. Higashi, T. (1990) *PROCESS: a program for indexing and processing R.-AXIS II imaging plate data*, Technical report, Rigaku Corp.
16. Brünger, A. T. (1992) *Nature 355*, 472−475.
17. Brünger, A. T. (1992) *X.-PLOR version 3.1. A system for X-ray crystallography and NMR*, Yale University Press, New Haven.
18. Jones, T. A., Zou, J. Y., Cowan, S. W., and Kjeldgaard, M. (1991) *Acta Crystallogr. A47*, 110−119.
19. Allen, F. H., and Kennard, O. (1993) *Chemical Design Automation News 8*, 31−37.
20. Wilson, A. J. C. (1949) *Acta Crystallogr. 2*, 318−321.
21. Read, R. J. (1986) *Acta Crystallogr. A42*, 140−149.
22. Maveyraud, L., Massova, I., Birck, C., Miyashita, K., Samama, J.-P., and Mobashery, S. (1996) *J. Am. Chem. Soc. 118*, 7435−7440.
23. Pratt, R. F. (1989) *Science 246*, 917−919.
24. Pratt, R. F., and Govardhan, C. P. (1984) *Proc. Natl. Acad. Sci. U.S.A. 81*, 1302−1306.
25. Mazzella, L. J., Pazhanisamy, S., and Pratt, R. F. (1991) *Biochem. J. 274*, 855−859.
26. Govardhan, C. P., and Pratt, R. F. (1987) *Biochemistry 26*, 3385−3395.
27. Richmonds, T. A., and Richards, J. H. (1993) *Protein Sci. 2 (Suppl. 1)*, 79 (poster 142-M).
28. Damblon, C., Raquet, X., Lian, L. Y., Lamotte-Brasseur, J., Fonzé, E., Charlier, P., Roberts, G. C., and Frère J.-M. (1996) *Proc. Natl. Acad. Sci. U.S.A. 93*, 1747−1752.
29. Gibson, R. M., Christensen, H., and Waley, S. G. (1990) *Biochem. J. 272*, 613−619.
30. Ellerby, L. M., Escobar, W. A., Fink, A. L., Mitchinson, C., and Wells, J. A. (1990) *Biochemistry 29*, 5797−5806.
31. Knap, A. K., and Pratt, R. F. (1991) *Biochem. J. 273*, 85−91.
32. Vijayakumar, S., Ravishanker, G., Pratt, R. F., and Beveridge, D. L. (1995) *J. Am. Chem. Soc. 117*, 1722−1730.
33. Kraulis, P. J. (1991) *J. Appl. Crystallogr. 24*, 946−950.
34. Wallace, A. C., Laskowski, R. A., and Thornton, J. M. (1995) *Protein Eng. 8*, 127−134.

BI972501B